Original Article

In vivo microcomputed tomography evaluation of rat alveolar bone and root resorption during orthodontic tooth movement

Nan Ru[a]; Sean Shih-Yao Liu[b]; Li Zhuang[c]; Song Li[d]; Yuxing Bai[d]

ABSTRACT

Objective: To observe the real-time microarchitecture changes of the alveolar bone and root resorption during orthodontic treatment.

Materials and Methods: A 10 g force was delivered to move the maxillary left first molars mesially in twenty 10-week-old rats for 14 days. The first molar and adjacent alveolar bone were scanned using in vivo microcomputed tomography at the following time points: days 0, 3, 7, and 14. Microarchitecture parameters, including bone volume fraction, structure model index, trabecular thickness, trabecular number, and trabecular separation of alveolar bone, were measured on the compression and tension side. The total root volume was measured, and the resorption crater volume at each time point was calculated. Univariate repeated measures analysis of variance with Bonferroni corrections were performed to compare the differences in each parameter between time points with significance level at $P < .05$.

Results: From day 3 to day 7, bone volume fraction, structure model index, trabecular thickness, and trabecular separation decreased significantly on the compression side, but the same parameters increased significantly on the tension side from day 7 to day 14. Root resorption volume of the mesial root increased significantly on day 7 of orthodontic loading.

Conclusions: Real-time root and bone resorption during orthodontic movement can be observed in 3 dimensions using in vivo micro-CT. Alveolar bone resorption and root resorption were observed mostly in the apical third on day 7 on the compression side; bone formation was observed on day 14 on the tension side during orthodontic tooth movement. (*Angle Orthod.* 2013;83:402–409.)

KEY WORDS: Micro-CT; Alveolar bone; Root resorption

INTRODUCTION

Although orthodontically induced root resorption (OIRR) during orthodontic treatment has been widely investigated for decades, the dynamic changes in microarchitecture of the alveolar bone and tooth root remain unclear. Different factors that affect alveolar bone and root resorption during orthodontic treatment have been studied, such as magnitude and duration of the force,[1] dental vulnerability,[2] age,[3] type of orthodontic appliance,[4] and direction of tooth movement.[5] With histologic staining and light microscopy or scanning electron microscopy, alveolar bone microarchitecture and OIRR can be observed in 2 dimensions.[6] However, these methods require sophisticated procedures with destruction of specimens and cannot be used to observe longitudinal changes in bone histomorphology. A new approach is needed to observe the real-time three-dimensional (3D) changes in the microstructure of alveolar bone and development of OIRR during tooth movement.

Microcomputed tomography (micro-CT), with a high resolution at 9 μm per pixel, can be used to observe the alveolar bone microarchitecture and detect the root resorption craters. Analogous to computed tomography, micro-CT is equipped with a microfocus X-ray tube that emits X-rays that are collimated and filtered

[a] PhD candidate, Department of Orthodontics, Capital Medical University School of Stomatology, Beijing, China.

[b] Assistant Professor of Orthodontics and Director, Mineralized Tissues and Histology Research Lab, and Director, Orthodontic Fellowship Program, Department of Orthodontics and Oral Facial Genetics, Indiana University School of Dentistry, IUPUI, Indianapolis, Ind.

[c] Lecturer, Department of Orthodontics, Capital Medical University School of Dentistry, Beijing, China.

[d] Professor, Department of Orthodontics, Capital Medical University School of Dentistry, Beijing, China.

Corresponding author: Dr Yuxing Bai, Department of Orthodontics, Capital Medical University School of Dentistry, Tiantan Xili 4, Chongwen District, Beijing, China 100050
(e-mail: byuxing@263.net)

Accepted: August 2012. Submitted: March 2012.
Published Online: October 3, 2012

to narrow the energy spectrum.[7] The X-rays pass through the object and are recorded by a two-dimensional charge-coupled device array. A micro-CT full scan involves a set of projections under different rotations of the object. The average resolution of micro-CT is sufficient for investigating such structures as mouse trabeculae because the width ranges from approximately 30 μm to 50 μm.[8] Moreover, in vivo micro-CT can observe the real-time changes in periodontal tissue without sacrificing the animal subjects.[9]

The objective of this study was to develop a new approach to observe real-time 3D changes of OIRR and alveolar bone microarchitectures during orthodontic tooth movement. In addition, 3D bone morphometric parameters were investigated to further understand dynamic responses in bone resorption and formation resulting from the compression and tension of the tooth root.

MATERIALS AND METHODS

Twenty 10-week-old male Sprague Dawley rats, specific pathogen free level 3, (SPF = 3) were acclimated for 1 week before the study. All animals were fed with a ground diet and water ad libitum. Procedures, housing, and animal care were approved by the Institutional Animal Care and Use Committee.

For each rat, after intraperitoneal injection of chloral hydrate (2 mL/kg), a cervical groove was prepared on the incisors using a round bur with a dental low-speed handpiece. A nickel-titanium (NiTi) coil spring 0.2 mm in diameter (IMD, Shanghai, China) was ligated between the maxillary left first molar and both incisors in each rat using a 0.08-inch ligature wire. The spring was activated for approximately 1 mm to produce a continuous force of 10 g to move the maxillary left first molar forward (Figure 1). The ligature wire was then secured with bond adhesive (Transbond, 3M Unitek, Monrovia, Calif) on the incisors. Spring retention was checked daily to ensure the stability of the applied force. The incisors, molar, and spring were cleaned and irrigated with tap water as needed to prevent potential trauma and irritation to the gingival and periodontal tissues.

After spring installation, the periodontal tissue of the mesial root of the maxillary first molar was scanned using a micro-CT system (SkyScan 1076, Kontich, Belgium) on days 0 (initiation), 3, 7, and 14. To avoid disturbing the micro-CT images, the rat was anesthetized and the NiTi spring was removed at each time point. The rat was placed in the animal holder, a carbon composite object bed (SkyScan), to secure the rat in a stable position, and the palate of the rat was adjusted parallel to the stage of the micro-CT. The rat's head was scanned at the resolution of 18 μm/pixel

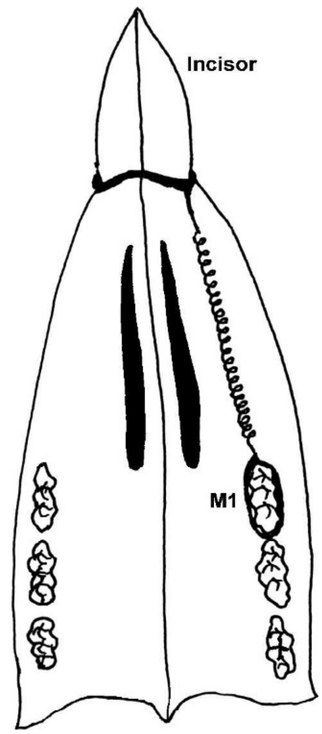

Figure 1. The nickel-titanium spring was ligated between the incisors and the maxillary left first molar in rats.

through 180° of rotation at 0.5° stepped increment at 2 s/degree. After scanning, the NiTi spring was reattached with a continuous force of 10 g. The average scanning time for each time point for each animal was approximately 40 minutes.

The raw data were further reconstructed to provide axial cross-section images using NRecon software, version 1.4.4 (Skyscan). Approximately 1000 axial cross-section images were collected per time point for each animal and images were converted into 16-bit bitmapped TIFF images with a resolution of 1024 × 1024 pixels.

Two 360 μm × 360 μm × 360 μm cubes of trabecular bone distal and mesial to the apical part of the mesial root of the maxillary left first molar were selected separately for analysis. The distance between the cube and the root was 500 μm (Figure 2A,B). Quantitative analysis was carried out using Analyser software, Version 1.12 (SkyScan). Three-dimensional microarchitecture parameters for trabecular bone were measured as follows: bone volume fraction (BV/TV), indicating the ratio of bone volume (BV) to total volume (TV); structure model index (SMI), varying from zero to three for ideal plate and rod structures; mean trabecular thickness (Tb.Th), indicating the local thickness at each voxel representing bone; trabecular number (Tb.N), indicating the inverse of the mean distance between the middle axes of the structure; and trabecular separation (Tb.Sp), indicating the direct

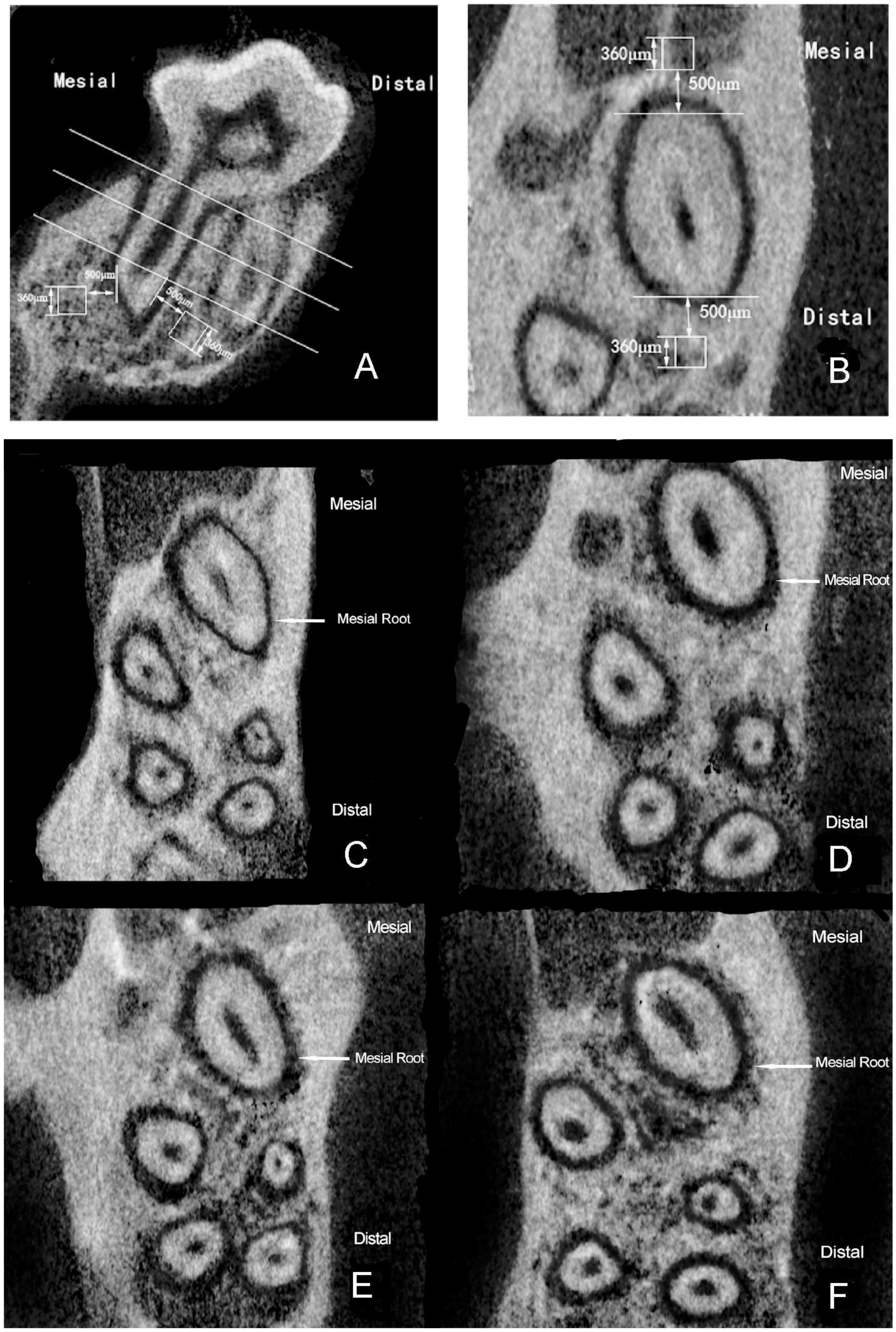

Figure 2. (A) Sagittal view of selected regions of interest in the alveolar bone adjacent to the apical third of the mesial root of the maxillary left first molar. (B) Horizontal view. (C) Axial cross-section images on day 0, (D) day 3, (E) day 7, and (F) day 14 of orthodontic loading.

thickness calculation to the non-bone portions of the 3D image.[1]

Using custom-designed software, the mesial root of the maxillary left first molar was segmented from the images. Based on a convex hull algorithm similar that of Harris et al.,[10] the total root volume was measured for each time point, and the root resorption crater volume on days 3, 7, and 14 was calculated by subtracting the root volume at each time point from the root volume on day 0.

Statistical Analysis

Using the Statistical Package for the Social Sciences, version 11.5 (SPSS Inc, Chicago, Ill), for each parameter, univariate repeated measures analysis of

Table 1. Microarchitecture Parameters for Trabecular Bone on the Compression Side of the Mesial Root of the Maxillary Left First Molar at Different Scanning Time Points in 20 Rats (mean ± standard deviation)

Microarchitecture Parameter	Day 0	Orthodontic Loading			F	P
		Day 3	Day 7	Day 14		
Bone volume fraction (BV/TV) (%)	69.10 ± 15.25[a]	63.70 ± 14.76[a]	41.34 ± 13.73[b]	31.20 ± 14.46[b]	4.975	.009[c]
Mean trabecular thickness (Tb.Th) (μm)	80.006 ± 19.938[a]	73.784 ± 17.451[a]	66.698 ± 10.182[b]	57.714 ± 8.466[b]	3.314	.040[c]
Trabecular number (Tb.N) (μm^{-1})	0.083 ± 0.009[a]	0.083 ± 0.015[a]	0.072 ± 0.011[a]	0.084 ± 0.012[a]	1.794	.179
Trabecular separation (Tb.Sp) (μm)	51.95 ± 11.08[a]	55.86 ± 9.91[a]	89.91 ± 30.08[b]	90.02 ± 19.52[b]	8.189	.001[c]
Structure model index (SMI)	0.464 ± 0.662[a]	0.505 ± 0.851[a]	1.508 ± 0.522[b]	1.834 ± 0.603[b]	12.207	<.001[c]

[a,b] Indicates that the value of two groups is significantly different ($P < .05$); [c] ($P < .05$).

variance was performed to compare the difference among days 0 (initiation), 3, 7, and 14 of orthodontic loading. Bonfferoni post hoc tests were used to compare the difference for paired time points. The significance level was set as $P < .05$.

RESULTS

Two-dimensional axial cross-section images of alveolar trabecular bone were shown at different time points (Figure 2C through F). On the compression (distal) side of the mesial root surface of the first molar, radiolucent areas, indicating reduced bone density and bone resorption, were shown on day 3 surrounding the widened periodontal ligament (PDL). From day 7 to day 14, the images showed that the PDL was narrowed with compression, and a greater radiolucent area, indicating increased bone resorption, was apparent. On the tension (mesial) side, however, the trabecular bone was shown to be radiopaque, indicating increased alveolar bone density, on days 7 and 14.

Three-dimensional microarchitecture parameters of trabecular bone on the compression side of the mesial root of the maxillary left first molar are summarized in Table 1 and Figure 3A, C, and E. The BV/TV and mean Tb.Th did not change from day 0 to day 3, but they decreased significantly from day 3 to day 7, and maintained a steady level between day 7 and day 14. There was no change in Tb.N over time. The Tb.Sp and SMI did not change from day 0 to day 3, but they increased significantly from day 3 to day 7 and plateaued until day 14.

Similarly, 3D microarchitecture parameters for trabecular bone on the tension are summarized in Table 2 and Figure 3B, D, and F. The BV/TV and Tb.Th did not change from day 0 to day 7, but they increased significantly from day 7 to day 14. There was no change in Tb.N over time. Although no changes were observed from day 0 to day 7, both Tb.Sp and SMI decreased significantly from day 7 to day 14.

Root resorption crater volume was calculated with three regions (cervical, middle, and apical third) divided from the root furcation to root apex (Figure 4). From day 0 to day 3, there was no obvious root resorption with smooth root surfaces (Figure 5A,B). Root resorption craters with well-defined margin occurred from day 7 to day 14 on the mesial and distal surfaces of the apical third (Figure 5C,D). Both wide shallow and deep resorption craters were mostly observed on the mesial surface. Scattered isolated lacunae were mainly seen on the distal surface of the root. Root resorption crater volume did not change from day 0 to day 3, but it increased significantly from day 3 to day 7 and plateaued until day 14 for the whole root and the apical third (Figure 5E,F).

DISCUSSION

Using 3D in vivo micro-CT, root resorption and reduced bone density on the compression side were observed on day 7 mostly in the apical third during orthodontic tooth movement with a 10 g of continuous force in rats. Similarly, others used coil springs to move the first molar orthodontically to investigate root resorption at different time points for 14 days.[11,12] Histologic studies showed that osteoclasts can be seen on the PDL-alveolar bone interface of the first molar without evident bone or root resorption on day 3 during orthodontic movement.[11–13] Some reported that undermining of bone resorption occurs on the surface of alveolar bone with slight root resorption on the mesial surface of the root on day 7.[13] However, others reported that the hyalinization appears first on day 7 on the surface of alveolar bone, and bone resorption occurs later on day 14.[11,13] In this study, a new method was used to investigate in vivo 3D real-time changes in root resorption and bone density and provide comparable observations on days 0, 3, 7, and 14 to previous histologic findings.

On the compression side, intensified radiolucency in the widened PDL on day 3 implies that osteoclasts were activated.[11–13] The BV/TV and Tb.Th significantly decreased on day 7 and day 14, which indicates rapid bone-density reduction, implying that a large amount of bone resorption occurred with possible high osteoclast activities. However, hyalinization was not observed using micro-CT. Hyalinization, if any, must have occurred before day 7, when undermining bone

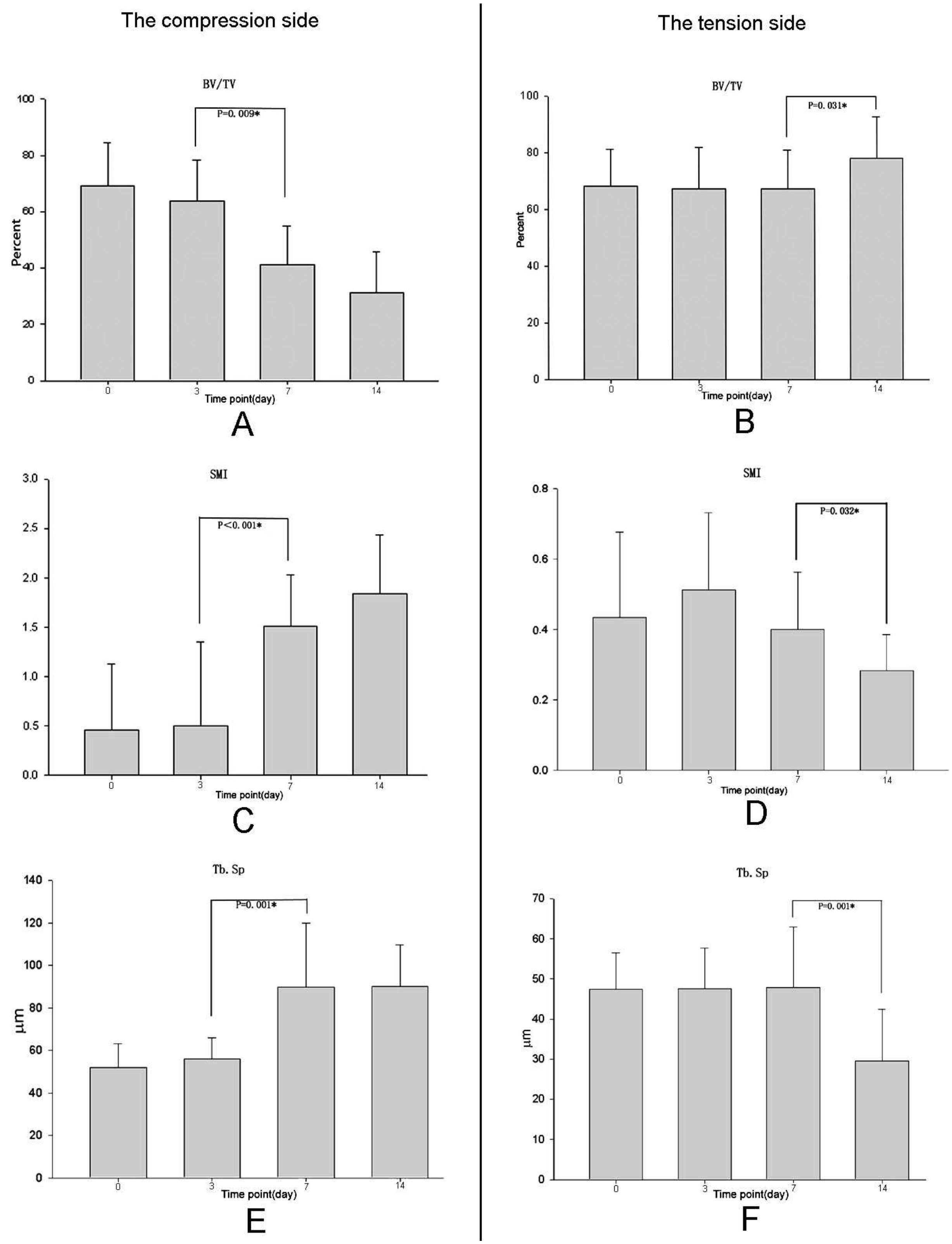

Figure 3. Bone volume fraction (BV/TV), structure model index (SMI), and trabecular separation (Tb.Sp) at different time points on the compression and the tension side. Error bars indicate standard deviations. $^*P < .05$.

Table 2. Microarchitecture Parameters for Trabecular Bone on the Tension Side of the Mesial Root of the Maxillary Left First Molar at Different Scanning Periods in 20 Rats (mean ± standard deviation)

Microarchitecture Parameter	Day 0	Orthodontic Loading Day 3	Orthodontic Loading Day 7	Orthodontic Loading Day 14	*F*	*P*
Bone volume fraction (BV/TV) (%)	68.22 ± 13.21[a]	67.23 ± 14.76[a]	67.34 ± 13.73[a]	78.20 ± 14.46[b]	6.483	.031[c]
Mean trabecular thickness (Tb.Th) (μm)	72.453 ± 10.904[a]	72.566 ± 9.787[a]	73.019 ± 9.083[a]	86.893 ± 9.792[b]	3.453	.032[c]
Trabecular number (Tb.N) (μm^{-1})	0.081 ± 0.008[a]	0.081 ± 0.014[a]	0.085 ± 0.011[a]	0.089 ± 0.012[a]	1.831	.181
Trabecular separation (Tb.Sp) (μm)	47.42 ± 9.16[a]	47.63 ± 10.02[a]	47.82 ± 15.07[a]	29.49 ± 12.96[b]	6.254	.011[c]
Structure model index (SMI)	0.435 ± 0.242[a]	0.512 ± 0.220[a]	0.400 ± 0.163[a]	0.283 ± 0.102[b]	8.467	.032[c]

[a,b] Indicates that the value of two groups is significantly different ($P < .05$); [c] ($P < .05$).

resorption occurred. With decreases in Tb.Th, no change in Tb.N indicates that osteoclasts induced bone resorption on the surface of the trabecular bone, leading to reduced bone density but the same trabecular number. Similarly, bone resorption on the trabecular surface caused increased distances between trabeculae, leading to significant increases in Tb.Sp from day 3 to day 7. The SMI is a method for determining the plate- or rod-like geometry of trabecular structures. An SMI score of 0 indicates plate-like structures and an SMI score of 3 indicates rod-like structures.[14] The increase in SMI from day 3 to day 7

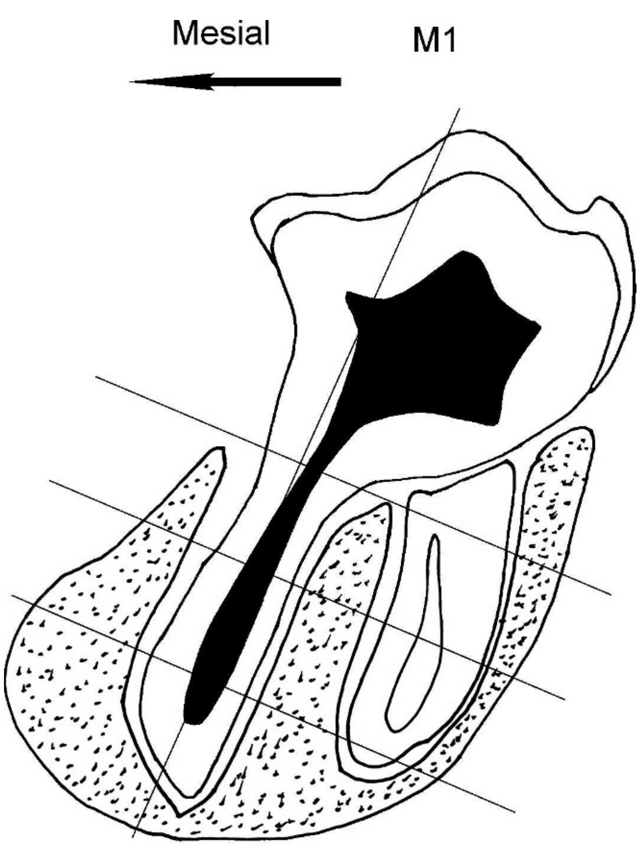

Figure 4. The mesial root divided into three regions from the root furcation to the root apex: cervical third, middle third, apical third.

demonstrated that the trabecular bone changed from plate-like to rod-like (loosen) bone structure.

On the tension side, BV/TV and Tb.Th increased significantly from day 7 to day 14, indicating that tension force induced bone formation. Interestingly, our findings showed that the bone formation was caused by increasing Tb.Th rather than Tb.N. The SMI decreased significantly from day 7 to day 14, indicating the trabecular bone changed from rod-like to plate-like (dense) bone structure.

Tooth movement consists of three phases: (1) compression of the viscoelastic PDL with alveolar bone bending for a few days, (2) a lag phase of hyalinization for 1 or 2 weeks, and (3) progressive movement with evident undermining bone resorption.[15,16] It is suggested that the limiting factor of tooth movement rate is to remove existing hyalinized tissue caused by direct or undermining bone resorption on the compression side.[12] Based on our findings, it is suggested that direct bone resorption occurred on day 3 in the PDL-alveolar bone interface, while undermining resorption occurred on day 7 in the alveolar bone adjacent to the PDL on the compression side. Once the tooth was moved to the resorptive region, bone formation occurred with thicken trabeculae on day 14 on the tension side.

Orthodontic tooth movement in this study was induced using a considerably light 10 g of continuous force. Previous studies suggest that applying a 10 g of force on the root surface area (24.91 mm^2) of the upper first molar in Sprague Dawley rats corresponds to approximately 100 g of force on the upper canine (43.2 g/cm^2) in humans.[17,18] Zhuang et al.[1] reported that both 30 g and 10 g forces caused a similar amount of root resorption; however, this might be because both forces were heavy, which exceeded physiologic conditions.

Most resorption occurred in the apical third of the root on day 7. Our results agreed with those of Chan et al.,[19] who found that root resorption occurred in the apical regions of the compression side. A greater amount of root resorption in the apical third was possibly caused by higher accumulated stress in this

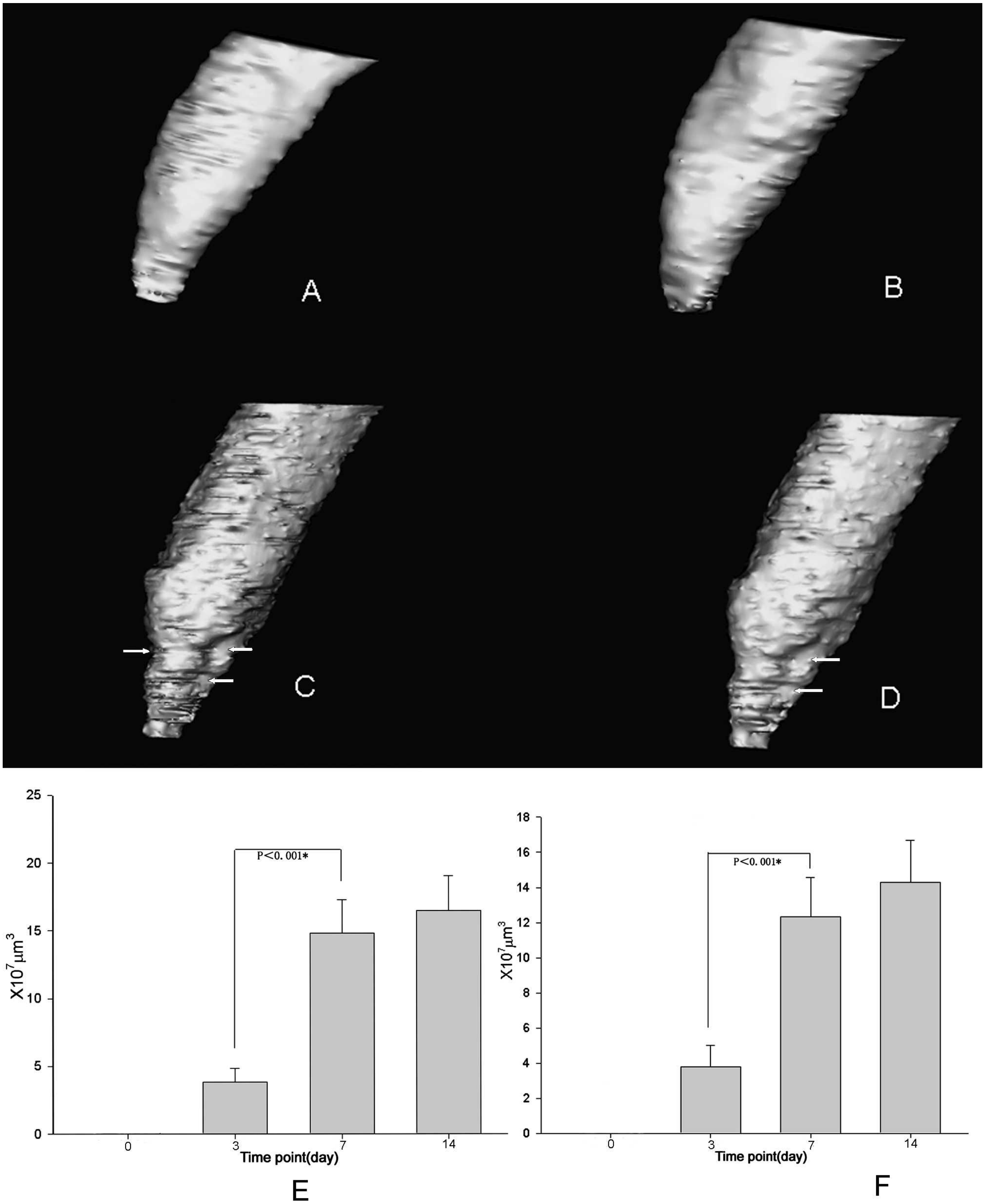

Figure 5. Reconstructed three-dimensional images of the mesial root on (A) day 0, (B) day 3, (C) day 7, and (D) day 14. White arrows indicate root lacunae. (E) Root resorption crater volume and (F) root resorption crater volume in the apical third at different time points. Error bars indicate standard deviations. *$P < .05$.

region. Using a biomechanical model and scanning electron microscopy, Casa et al.[20] confirmed that root resorption occurred at zones of maximum stress when sliding the premolar distally in humans. Applying a higher force magnitude on the tooth induced a significantly greater amount of root resorption. A previous finite element model showed that when moving the upper left first molar in rats, the tooth was tipped mesially and extruded and force was accumulated at the root apex.[21] This might explain why root resorption occurred mostly in the apical region.

CONCLUSIONS

- Real-time root resorption during orthodontic movement was observed in three dimensions using in vivo micro-CT.
- With a light 10 g orthodontic force, bone resorption occurred on the compression side on day 7 and bone formation occurred on the tension side on day 14.
- Most root resorption was observed in the apical third of the mesial root on day 7.

ACKNOWLEDGMENTS

Appreciation is expressed to Dr Barry H Grayson for the manuscript revision and to IMD Inc for providing the data for the coil springs.

REFERENCES

1. Li Zhuang, Yuxing Bai, Xianying Meng. Three-dimensional morphology of root and alveolar trabecular bone during tooth movement using micro-computed tomography. *Angle Orthod*. 2011;81:420–425.
2. Mirabella AD, Artun J. Risk factors for apical root resorption of maxillary anterior teeth in adult orthodontic patients. *Am J Orthod Dentofacial Orthop*. 1995;108:48–55.
3. Mavragani M, Boe OE, Wisth PJ, Selvig KA. Changes in root length during orthodontic treatment: advantages for immature teeth. *Eur J Orthod*. 2002;24:91–97.
4. Pandis N, Nasika M, Polychronopoulou A, Eliades T. External apical root resorption in patients treated with conventional and self-ligating brackets. *Am J Orthod Dentofacial Orthop*. 2008;134:646–651.
5. Janson GR, De Luca Canto G, Martins DR, Henriques JF, De Freitas MR. A radiographic comparison of apical root resorption after orthodontic treatment with 3 different fixed appliance techniques. *Am J Orthod Dentofacial Orthop*. 2000;118:262–273.
6. Jones SJ, Boyde A. A study of human root cementum surfaces as prepared for and examined in the scanning electron microscope. *Cell Tissue Res*. 1972;130:318–337.
7. Stauber M, Muller R. Microcomputed tomography: a method for the non-destructive evaluation of the three-dimensional structure of biological specimens. *Methods Mol Biol*. 2008;455:273–292.
8. Martin-Badosa E, Amblard D, Nuzzo S, Elmoutaouakkil A, Vico L, Peyrin F. Excised bone structures in mice: imaging at three-dimensional synchrotron radiation micro CT. *Radiology*. 2003;229:921–928.
9. Nakamura Y, Noda K, Shimoda S, Oikawa T, Arai C, Nomura Y, Kawasaki K. Time-lapse observation of rat periodontal ligament during function and tooth movement, using micro-computed tomography. *Eur J Orthod*. 2008;30:320–326.
10. Harris DA, Jones AS, Darendeliler MA. Physical properties of root cementum: part 8. Volumetric analysis of root resorption craters after application of controlled intrusive light and heavy orthodontic forces: a microcomputed tomography scan study. *Am J Orthod Dentofacial Orthop*. 2006;130:639–647.
11. Tomizuka R, Shimizu Y, Kanetaka H, Suzuki A, Urayama S, Kikuchi M, Mitani H, Igarashi K. Histological evaluation of the effects of initially light and gradually increasing force on orthodontic tooth movement. *Angle Orthod*. 2007;77:410–416.
12. Kohno T, Matsumoto Y, Kanno Z, Warita H, Soma K. Experimental tooth movement under light orthodontic forces: rates of tooth movement and changes of the periodontium. *J Orthod*. 2002;29:129–135.
13. Verna C, Zaffe D, Siciliani G. Histomorphometric study of bone reactions during orthodontic tooth movement in rats. *Bone*. 1999;24:371–379.
14. Hildebrand T, Rüegsegger P. A new method for the model-independent assessment of thickness in three-dimensional images. *J Microsc*. 1997;185:67–75.
15. Storey E. The nature of tooth movement. *Am J Orthod*. 1973;63:292–314.
16. King GJ, Fishlschweiger W. The effect of force magnitude on extractable bone resorptive activity and cemental cratering in orthodontic tooth movement. *J Dent Res*. 1982;61:775–779.
17. Gonzales C, Hotokezaka H, Yoshimatsu M, Yozgatian JH, Darendeliler MA, Yoshida N. Force magnitude and duration effects on amount of tooth movement and root resorption in the rat molar. *Angle Orthod*. 2008;78:502–509.
18. Noda K, Nakamura Y, Kogure K, Nomura Y. Morphological changes in the rat periodontal ligament and its vascularity after experimental tooth movement using superelastic forces. *Eur J Orthod*. 2009;31:37–45.
19. Chan E, Darendeliler MA. Physical properties of root cementum: part 7. Extent of root resorption under areas of compression and tension. *Am J Orthod Dentofacial Orthop*. 2006;129:504–510.
20. Casa MA, Faltin RM, Faltin K, Sander FG, Arana-Chavez VE. Root resorptions in upper first premolars after application of continuous torque movement. *J Orofac Orthop*. 2001;62:285–295.
21. Rudolph DJ, Willes PMG, Sameshima GT. A finite element model of apical force distribution from orthodontic tooth movement. *Angle Orthod*. 2001;71:127–131.